The Journal of Immunology

Exploiting Pre-Existing CD4+ T Cell Help from Bacille Calmette–Guérin Vaccination to Improve Antiviral Antibody Responses

This information is current as of January 2, 2021.

Tony W. Ng, Ariel S. Wirchnianski, Anna Z. Wec, J. Maximilian Fels, Christopher T. Johndrow, Kevin O. Saunders, Hua-Xin Liao, John Chan, William R. Jacobs, Jr., Kartik Chandran and Steven A. Porcelli

---

Exploiting Pre-Existing CD4+ T Cell Help from Bacille Calmette–Guérin Vaccination to Improve Antiviral Antibody Responses

Tony W. Ng,* Ariel S. Wirchnianski,* Anna Z. Wec,*,† J. Maximilian Fels,*
Christopher T. Johndrow,* Kevin O. Saunders,‡ Hua-Xin Liao,‡ John Chan,*,§
William R. Jacobs, Jr.,* Kartik Chandran,* and Steven A. Porcelli*,§

The continuing emergence of viral pathogens and their rapid spread into heavily populated areas around the world underscore the urgency for development of highly effective vaccines to generate protective antiviral Ab responses. Many established and newly emerging viral pathogens, including HIV and Ebola viruses, are most prevalent in regions of the world in which *Mycobacterium tuberculosis* infection remains endemic and vaccination at birth with *M. bovis* bacille Calmette–Guérin (BCG) is widely used. We have investigated the potential for using CD4+ T cells arising in response to BCG as a source of help for driving Ab responses against viral vaccines. To test this approach, we designed vaccines comprised of protein immunogens fused to an immunodominant CD4+ T cell epitope of the secreted Ag 85B protein of BCG. Proof-of-concept experiments showed that the presence of BCG-specific Th cells in previously BCG-vaccinated mice had a dose-sparing effect for subsequent vaccination with fusion proteins containing the Ag 85B epitope and consistently induced isotype switching to the IgG2c subclass. Studies using an Ebola virus glycoprotein fused to the Ag 85B epitope showed that prior BCG vaccination promoted high-affinity IgG1 responses that neutralized viral infection. The design of fusion protein vaccines with the ability to recruit BCG-specific CD4+ Th cells may be a useful and broadly applicable approach to generating improved vaccines against a range of established and newly emergent viral pathogens. *The Journal of Immunology*, 2020, 205: 425–437.

Recent outbreaks of pathogenic viruses, such as Ebola, Chikungunya, and Zika viruses, have resulted in increased morbidity and mortality surpassing past outbreaks [1]. Factors that contribute to the severity of current outbreaks include human population growth, urbanization with extension into habitats that harbor viral reservoirs, and the increased mobility with modern transportation that facilitates the spread of infections [2]. To contain or prevent future outbreaks, there is an urgent need to develop antiviral vaccines as a rapid, efficient, and cost-effective

intervention. Basic knowledge on the features of protective immune responses has been greatly amplified by studies of the most recent Ebola virus (EBOV) outbreaks, and also by the HIV vaccine trial (RV144) in Thailand [3, 4]. These studies have emphasized the relevance of neutralizing Abs [5] and also Abs that recruit effector functions such as Ab-dependent cellular cytotoxicity (ADCC) [6]. In general, the induction of such Abs is dependent on the binding of specific Ags by BCRs, an important step that facilitates efficient internalization of the immunogen into MHC class II (MHCII) compartments for generation of peptides and their loading onto MHCII molecules for presentation to Th [7, 8]. This cognate interaction between B and Th cells is known as linked recognition, a concept derived from studies with hapten-carrier fusion proteins in which the production of anti-hapten Abs from B cells with BCRs that initially recognize the poorly immunogenic hapten is driven by help from T cells that are specific for the carrier protein to which it is linked [9]. Fusion protein vaccines based on this principle are often used to promote Ab responses to polysaccharides, as in the case with infant immunization against bacterial pathogens containing carbohydrate capsules [10, 11], or other molecules that fail to elicit effective Abs because of suboptimal Th responses [12, 13].

Besides the cognate interaction between B and Th cells, cytokines and costimulatory molecules from distinct Th subsets also contribute significantly to the development of Ab responses, especially those against viral infections. For example, extrafollicular Th1 cells promote the development of short-lived plasmablasts that produce Abs with little somatic hypermutation and thus have low affinity toward their Ags. Nevertheless, such Abs contribute significantly to early protective immunity, especially against viral pathogens such as influenza A [14]. The development of these Abs is influenced by IFN-γ secreted from Th1 cells that drives isotype

*Department of Microbiology and Immunology, Albert Einstein College of Medicine, Bronx, NY 10461; †Adimab, Lebanon, NH 03766; ‡Department of Medicine, Duke University School of Medicine, Durham, NC 27710; and §Department of Medicine, Albert Einstein College of Medicine, Bronx, NY 10461

ORCIDs: 0000-0002-2460-7929 (T.W.N.); 0000-0002-2134-2152 (A.Z.W.); 0000-0003-3321-3080 (W.R.J.).

Address correspondence and reprint requests to Dr. Steven A. Porcelli, Department of Microbiology and Immunology, Albert Einstein College of Medicine, Forchheimer Building, Room 416, 1300 Morris Park Avenue, Bronx, NY 10461. E-mail address: steven.porcelli@einsteinmed.org

The online version of this article contains supplemental material.

Abbreviations used in this article: ADCC, Ab-dependent cellular cytotoxicity; Δ85B BCG, Ag85B-deleted BCG strain; BCG, bacille Calmette–Guérin; CatS, cathepsin S; EBOV, Ebola virus; EBOV GP, EBOV glycoprotein; GuHCl, guanidine hydrochloride; IU, infectious unit; mDC, murine dendritic cell; MHCII, MHC class II; NTh, N terminus Th; PBST, PBS with 0.05% Tween 20; pNTh, NTh plasmid; RT, room temperature; rVSV, recombinant vesicular stomatitis virus; TCH, T cell hybridoma; Tfh, follicular helper T cell; Tg, transgenic; WT, wild-type.

switching to Ab subclasses that control viral infection through mechanisms that include Fc receptor–dependent functions such as ADCC (15–17). In contrast, for long term protection, the interaction between follicular helper T cells (Tfh) and B cells promotes the development of long-lived plasma cells capable of secreting large amounts of high-affinity Abs. These Abs, which have important neutralizing effects in viral infections, arise predominantly from B cells in germinal centers (GCs), where interactions with Tfh drive somatic hypermutation and affinity maturation (18, 19). Thus, different Th subsets play critically important and complementary roles in the generation of both rapidly protective and long-lived protective Abs.

With a proven track record of safety and its ability to confer partial protection against childhood tuberculous, meningitis, and miliary disease (20), bacille Calmette–Guérin (BCG) is administered routinely in countries with high prevalence of tuberculosis as a universal vaccine for newborns (21). BCG-vaccinated individuals develop mycobacteria-specific CD4⁺ Th cells that persist as long-lived memory cells for decades (22, 23). Although much emphasis has been placed on the Th1 response to mycobacteria (24–27), other Th subsets have been described in BCG vaccination and in *Mycobacterium tuberculosis*) infection, all which have the potential to promote humoral immune responses (18, 26, 28–31). This raises the possibility of using pre-existing BCG-specific Th cells in BCG-immunized individuals to drive Ab production against appropriately engineered viral immunogens as a vaccination strategy. To test this in a preclinical mouse model, we developed model vaccine subunits in which the B cell immunogen was fused with a known immunodominant CD4⁺ T cell epitope of BCG. In this study, we show that mice primed with BCG developed BCG-specific Th cell subsets that could be recruited by such subunit vaccines to drive Ab responses, resulting in accelerated and increased Ab production. BCG-specific Th cells were induced by BCG vaccination in neonatal mice, and their contribution to Ab responses in vaccination persisted in adult animals. Our analysis showed that Abs facilitated by BCG-specific Th cells had enhanced capacity for neutralizing virus entry into host cells, which correlated with increased Ab affinity in the IgG1 subclass. Abs that were class switched to IgG2c were also consistently detected, suggesting the potential for other relevant effector functions such as ADCC. Overall, our findings provide an initial proof-of-concept for a practical approach to improving antiviral vaccines by designing immunogens that can use pre-existing BCG-specific Th cells to promote protective Ab responses.

Materials and Methods
Mice

Five-week-old female wild-type (WT) C57BL/6J mice were obtained from The Jackson Laboratory (Bar Harbor, ME), and 5-d-old C57BL/6 mice were bred in our facility using parental mice obtained from The Jackson Laboratory. GFP⁺ C57BL/6-P25 TCR-transgenic (Tg) mice that recognize the I-Aᵇ–restricted CD4⁺ T cell epitope from the immunodominant mycobacterial Ag Ag85B (15-mer peptide FQDAYNAAGGHNAVF) were bred in our facility by crossing P25-TCR-Tg mice (32, 33) (gift from Dr. J.D. Ernst; University of California San Francisco, San Francisco, California) with GFP-expressing Tg mice (strain C57BL/6-Tg(UBC-GFP) 30Scha/J) obtained from The Jackson Laboratory. All mice were maintained in specific pathogen–free conditions in compliance with regulations established by the Albert Einstein College of Medicine Institutional Animal Use and Care and Institutional Biosafety Committees. All procedures involving the use of these animals were performed according to protocols approved by the Albert Einstein College of Medicine Institutional Animal Care and Use Committee.

Mycobacterial strains and vaccinations

BCG Danish strain (Statens Serum Institute, Copenhagen, Denmark) was the parental strain used in this study. The Ag85B-deleted BCG strain (Δ85B

BCG) was constructed by deleting the *fbpb* gene encoding Ag85B through allelic exchange with a shuttle phasmid containing flanking sequences for promoting allelic exchange (gift from Dr. J.D. Ernst; University of California, San Francisco) using the specialized phage transduction method as described previously (34). Colonies of Δ85B BCG were selected for hygromycin resistance following transduction, and the *fbpb* deletion was confirmed by PCR analysis of genomic DNA with primers TN33 (5′-GCGGGATCCCATGACAGACGTGAGCCGAAAG-3′), TN34 (5′-GCGAAGCTTGCCGGCGCCTAACGAACTCTGC-3′), TN46 (5′-GG-AAAACCTTCCTGACCAGCGAGC-3′), and TN47 (5′-CGGCGCGGA-CAGCAAACTCCAGTG-3′) as described in Supplemental Fig. 1A. The complemented strain (Δ85B::*fbpb*) was generated by transformation with plasmid pMV261 containing the full length sequence of *fbpb* and selecting for kanamycin resistance. BCG and derivatives were grown in Sauton medium, with antibiotics for selection when appropriate (35). Bacteria were grown from low-passage-number frozen stocks, cultured to midlog phase, centrifuged at $600 \times g$ for 10 min, and resuspended in sterile PBS (Thermo Fisher Scientific, Waltham, MA) prior to injection into mice. For vaccination, all BCG strains were administered to 5-d- or 5-wk-old mice by s.c. injection at the scruff of the neck. Dose was 1×10^5 CFU for 5 d old or 1×10^7 CFU for 5-wk-old animals. For recombinant protein vaccine injections, the vaccine in PBS was mixed in a 1:1 volume ratio with alum (Imject Alum; Thermo Fisher Scientific) to a final indicated concentration ranging from 10 to 0.1 μg/ml. One hundred microliters of this vaccine mixture was administered i.m. into the mouse through the thigh muscles with 50 μl per hind limb to provide final doses ranging from 1 to 0.01 μg of the recombinant fusion protein vaccine per mouse.

Primary cell culture and cell lines

Vero cells were from the American Type Culture Collection and were maintained in high-glucose DMEM (Thermo Fisher Scientific). FreeStyle 293-F cells (Thermo Fisher Scientific) were maintained in Life Technologies FreeStyle 293 Expression Medium with GlutaMAX (Thermo Fisher Scientific). Murine T cell hybridomas (TCHs) specific for I-Aᵇ–restricted CD4 T cell epitopes of Ags used in this work were generated using a previously reported method (36). For the generation of TCH specific for the Ag85B, CD4⁺ T cells were isolated from splenocytes of P25-TCR-Tg mice (32, 33). For the generation of TCH specific for the TB9.8, CD4⁺ T cells were derived from splenocytes of C57BL/6 mice immunized s.c. with BCG (1×10^7 CFU), and boosted 4 wk later with the same dose of BCG administered i.v., followed 2 d later by isolation of CD4⁺ T cells from splenocytes. Purified CD4⁺ T cells were fused with the BW5147.G.14 mouse lymphoma cell line (ATCC TIB-48; American Type Culture Collection). Following fusion, the Ag85B- and TB9.8-specific TCHs were isolated by screening for reactivity to the peptides corresponding to epitopes P25 (FQDAYNAAGGHNAVF) and P10 (ESSAAFQAAHARFVAA) from Ag85B and TB9.8, respectively. These TCHs were maintained in complete RPMI medium (RPMI 1640 supplemented with 10 mM HEPES, 50 μg/ml penicillin/streptomycin, 55 μM 2-ME [Thermo Fisher Scientific], and 10% heat-inactivated [56°C, 30 min] FBS [Atlanta Biologicals, Flowery Branch, GA]). Murine bone marrow dendritic cells were derived as previously described (37) and cultured in RPMI 1640 with murine GM-CSF (20 ng/ml) (PeproTech).

Plasmid construction

The sequence of the N terminus Th (NTh) fragment containing the human Ig κ signal sequence followed by a hexahistidine tag, thrombin cleavage site, and BCG-derived CD4⁺ T cell epitopes P25 and P10 separated by cathepsin S (CatS) cleavage sites, was synthesized using codon optimization for mammalian expression (GenScript, Piscataway, NJ). The *ova* gene encoding chicken OVA was amplified from OVA plasmid [plasmid number 31598, a gift from Dr. S. Levy; Addgene (38)], using primers TN199 (5′-GCGCTCGAGGGCTCCATCGGCGCAGCAAGC-3′) and TN200 (5′-GCGTCTAGAGGGGGGAAACACATC-3′) and subcloned into pcDNA3.1/Hygro expression vector (Thermo Fisher Scientific) via the XhoI–XbaI sites. To construct the NTh plasmid (pNTh) OVA, the NTh fragment was cloned in-frame into the N terminus of the *ova* gene in pcDNA3.1 via the BamHI and XhoI sites (Supplemental Fig. 2). To construct plasmid P25-NTh OVA with a single BCG-specific CD4⁺ T cell epitope or plasmid WT OVA that lacks BCG CD4⁺ T cell epitopes, inverse PCR primer pair TN235 (5′-CTCGAGGGCTCCATCGGC-3′) and TN236 (5′-TAGTCCGACTGTAAACACGGC-3′) for plasmid P25-NTh OVA or TN214 (5′-ACAGTCGGTCTGCTCGAG-3′) and TN215 (5′-GC-TCCCCTAGGCACGAG-3′) for plasmid WT OVA were used to delete the corresponding BCG-specific CD4⁺ T cell epitope(s) from pNTh OVA. For the NTh version of the EBOV glycoprotein (EBOV GP), the NTh fragment

was amplified from pNTh OVA with primers TN231 (5′-CGCACCGG-TACCGTGGGTCTGTTCCAGGAC-3′) and TN232 (5′-CGCACCGGT-CAGACCGACTGTTGCTGCGAC-3′) to introduce AgeI sites for cloning into the pHLsec-EGP-WT plasmid that contains the EBOV GP. The design of the EBOV GP (UniProt entry KB-Q05320) was based on the version used in a previously published crystal structure that lacks the mucin domain (aa 313–463), and its transmembrane domain was replaced by a foldon trimerization domain and a 6× His tag (39). A synthesized DNA fragment corresponding to the above glycoprotein, with the addition of a A42T mutation to restore to the N-40 glycan, was subcloned into the pHLsec expression vector (40) using the restriction sites AgeI and KpnI. All plasmids encoding the fusion proteins were purified from DH5α strain of *Escherichia coli* using the EndoFree Plasmid Maxi Kit (QIAGEN, Germantown, MD).

Recombinant protein expression and purification

For recombinant protein expression, transfection was performed by mixing 400 μg of DNA with 1200 μl of 1 mg/ml PEI MAX transfection reagent (Polysciences, Warrington, PA) in 45 ml of PBS and added into a 2-l flask containing 1×10^6 FreeStyle 293-F cells (Thermo Fisher Scientific) in 600 ml of Life Technologies FreeStyle 293 Expression Medium with GlutaMAX (Thermo Fisher Scientific). The flask was kept in a shaker set at 125 rpm and incubated at 37°C with 8% CO_2 for 5 d. Cells were removed by centrifugation at $800 \times g$. For purification of rOVA and EBOV GP, imidazole was added to 30 mM to the supernatant for purification of the hexahistidine-tagged fusion protein proteins using a 5 ml HisTrap HP column (GE Healthcare Life Sciences, Pittsburgh, PA). Recombinant proteins were eluted with 500 mM imidazole and passed through Amicon Ultra Centrifugal Filter Units (Millipore Sigma, Burlington, MA) with a 30-kDa molecular mass cut-off to allow buffer exchange into PBS. Buffer exchange into PBS and concentration of the purified protein was carried out using Vivaspin 20 concentrators (Sartorius, Goettingen, Germany). All recombinant proteins were purified and concentrated under endotoxin free conditions. Protein concentrations of the purified recombinant proteins were determined by bicinchoninic acid assay (Thermo fisher Scientific, Rockford, IL), and aliquots were stored at −80°C until day of use.

SDS-PAGE analysis of fusion proteins

Purified fusion protein Ags or vaccines were subjected to SDS-PAGE followed by staining with GelCode Blue Safe Protein Stain (Thermo Fisher Scientific) for direct visualization of protein bands or by transferring to nitrocellulose membranes for immunoblotting. After blocking with 5% milk in PBS with 0.05% Tween 20 (PBST), nitrocellulose membranes containing NTh EBOV fusion protein vaccine were incubated with either rabbit anti–EBOV GP1 (3) or human anti–EBOV GP2 (41), and nitrocellulose membranes containing the OVA version of the fusion protein vaccine were incubated with rabbit anti-SIINFELK (Covance, Denver, PA). HRP-conjugated goat anti-rabbit or anti-human Abs (SouthernBiotech, Birmingham, AL) were used as detection Abs, followed by the addition of the SuperSignal West Pico PLUS Chemiluminescent Substrate (Thermo Fisher Scientific).

ELISA and ELISPOT assays for cytokine secretion

Capture ELISA was used to measure cytokine responses from mouse TCHs or splenocytes. Mouse TCHs specific to the peptide P25 of Ag85B, peptide P10 of TB9.8, or peptide P72 of isocitrate lyase were cocultured in complete RPMI 1640 with murine bone marrow–derived dendritic cells in the presence of the fusion protein vaccine (10 μg/ml), individual peptide controls (5 μg/ml), or BCG strains (multiplicity of infection of 10) at 37°C for 18 h. Similarly, splenocytes from mice vaccinated with BCG strains were cultured in complete RPMI 1640 in the presence of peptide-25 (5 μg/ml) or H37Rv lysate (10 μg/ml) at 37°C for 18 h. Supernatants were assayed for IL-2 or IFN-γ using capture and biotin-labeled detection Ab pairs (BD Biosciences, Franklin Lakes, NJ). Detection was performed with HRP-conjugated streptavidin (BD Biosciences) and Turbo TMB substrate (Thermo Fisher Scientific), and absorbance was measured with a Wallac 1420 VICTOR2 microplate reader (Perkin Elmer, Waltham, MA).

A standard ELISA was performed to detect Ag-specific Abs in sera from vaccinated mice. Blood samples from vaccinated mice were collected through retro-orbital bleed and allowed to clot for 20 min at room temperature (RT). Serum was removed from cells by centrifuging at $2000 \times g$ for 10 min at RT and kept at −80°C for storage. Corning 96-Well EIA/RIA Assay Microplates (Thermo Fisher Scientific) were coated with 5 μg per well of purified OVA (Worthington Biochemical, Lakewood, NJ) or HIV gp120 in sodium bicarbonate buffer (15 mM Na_2CO_3, 34 mM $NaHCO_3$ [pH 9.5]) overnight at 4°C, or with ∼95,000 infectious units (IU) of

recombinant vesicular stomatitis virus (rVSV) expressing EBOV GP (rVSV-EBOV) in PBS (pH 7.4) overnight at 4°C. The Ag-coated ELISA plate was washed three times with PBST and blocked with 5% milk in PBST for 45 min at RT. Serum samples were then incubated with the Ag-coated ELISA plate for 2 h at RT, washed four times with PBST, and incubated with HRP-conjugated mouse IgG1- or IgG2c-specific Abs (SouthernBiotech) for 1 h at RT. After washing four times with PBST, the signal was detected with the SIGMAFAST OPD substrate (Sigma-Aldrich, St. Louis, MO), and the absorbance was measured with the Wallac 1420 Victor2 microplate reader (Perkin Elmer). To measure the affinity of Ag–Ab interaction, a guanidine hydrochloride (GuHCl)–modified ELISA was performed (42). After incubating the serum samples with the Ag-coated ELISA plate and subsequent PBST washes, the ELISA plate was either treated with PBS or 2.5 M GuHCl for 15 min at ∼22°C. The plates were then washed three times with PBST, followed by incubation with HRP-conjugated mouse IgG1- or IgG2c-specific Abs (SouthernBiotech) and continuation of the standard ELISA procedure mentioned above.

For ELISPOT assays, 5-wk-old female WT C57BL/6J mice were vaccinated with PBS, BCG, or revaccinated with BCG after a 5-wk interval at a dose of 1×10^7 CFU. Five weeks after the last vaccination, spleens were harvested, and CD4+ T cells were purified by negative selection using a commercially available kit and following the manufacturer's instruction (Miltenyi Biotec, Auburn, CA). ELISPOT plates (Millipore Sigma) were coated with 50 μl per well of 10 μg/ml anti-IFN-γ (clone R4-6A2), 4 μg/ml anti-IL-4 (clone OX-81), 4 μg/ml anti-IL-17A (clone TC11-18H10) (BD Biosciences), or 10 μg/ml anti-IL-21 (Thermo Fisher Scientific) as capture Abs for 18 h at 4°C. Plates were washed and blocked with RPMI 1640 (Thermo Fisher Scientific) containing 2% FBS for 2 h at RT. A total of 2×10^5 purified CD4+ T cells along with 5×10^5 splenocytes from naive mice as APCs, were plated with Ag85B (P25) peptide (FQDAY-NAAGGHNAVF; 10 μg/ml) (Mimotopes, Mulgrave, VIC, Australia) or *M. tuberculosis* H37Rv bacterial lysate (10 μg/ml) (BEI Resources, Manassas, VA) or no Ag in 100 μl of complete RPMI 1640 medium for 36 h at 37°C. After cells were removed, plates were washed with PBST, and 50 μl per well of 1 μg/ml of biotinylated Abs (anti-IFN-γ [clone XMG1.2], anti-IL-4 [clone B11-3], anti-IL-17A (clone TC11-8H4) (BD Biosciences), or anti-IL-21 (Thermo Fisher Scientific) as detection Abs were added and incubated for 2 h at 37°C, followed by washing with PBST. Fifty microliters per well of streptavidin–alkaline phosphatase at 1:1000 in PBS (Sigma-Aldrich) was added to the plates for 1 h at 37°C followed by washing and addition of the BCIP/NBT substrate (Sigma-Aldrich). The reaction was stopped by washing the wells with water, and spots were counted using an automated ELISPOT reader (Autoimmun Diagnostika GmbH, Strasbourg, Germany).

Flow cytometry analysis of Th subsets

Five-week-old female WT C57BL/6J mice were vaccinated with PBS or BCG by s.c. route at 1×10^7 CFU per mouse. Five weeks after vaccination, splenocytes were isolated, treated with RBC lysis buffer, cultured in complete RPMI 1640 medium as described above, and stimulated for 2 h with mycobacteria Ags (peptide P25 or H37Rv lysate) as mentioned above, followed by another 6 h of Ag stimulation in the presence of monensin (5 μM) and brefeldin A (5 μg/ml) (Sigma-Aldrich). Afterward, cells were resuspended in PBS and stained with Molecular Probes LIVE/DEAD Fixable Blue Dead Cell Stain (Thermo Fisher Scientific) viability dye and subsequently with fluorochrome-conjugated Abs against surface markers in FACS buffer (PBS with 2% FBS and 0.05% sodium azide). Following surface staining, cells were fixed in PBS containing 2% paraformaldehyde (Electron Microscopy Sciences, Hatfield, PA), permeabilized with eBioscience Fixation and Permeabilization Buffer (Thermo Fisher Scientific), and stained for intracellular cytokines and transcription factors. The following Abs were used for staining: CD4 allophycocyanin–H7 (clone GK1.5), B220 PE–Cy5 (clone RA3-6B2), IFN-γ Alexa Fluor 700 (clone XMG1.2), Bcl-6 Alexa Fluor 647 (clone K112-91), CXCR5 PE–CF594 (clone 2G8), RORγT PE–CF594 (clone Q31-378) (BD Biosciences), MHCII PE–Cy5 (clone M5/114.15.2), IL-21 (clone FFA21), T-bet PE–Cy7 (clone eBio4B10), GATA-3 Alexa Fluor 488 (clone TWAJ) (Thermo Fisher Scientific), and CD8α PE–Cy5 (clone 53-6.7) (Tonbo Biosciences, San Diego, CA). Flow cytometry was performed with the BD Biosciences LSRII Flow Cytometer configured with five lasers, and 2×10^5 events per sample were collected and analyzed using FlowJo software (BD Biosciences).

Adoptive transfer of P25 Tg CD4+ T cells

Naive CD4+ T cells from P25 TCR-Tg/GFP mice were purified by negative selection with the Miltenyi Biotec Negative Selection Kit as mentioned above, with slight modification by adding anti-CD44 conjugated to biotin

(clone IM7) (Thermo Fisher Scientific) to remove small numbers of memory T cells that are present in these animals. Purified CD4$^+$ T cells (4×10^4 in 100 μl of PBS) were injected i.v. into WT C57BL/6 mice. Sixteen hours later, 5×10^6 CFU of BCG were administered in a volume of 100 μl of PBS s.c. at the base of the tail. On day 7 after vaccination, mice were euthanized, and spleens were harvested and analyzed by FACS. Tissues were also fixed in 10% neutral buffered formalin, paraffin embedded, and sectioned. Ag retrieval with 10 mM Na citrate (pH 6) was performed. Sections were blocked in 5% donkey serum/2% BSA and stained with rabbit anti-GFP Ab (A11122; Thermo Fisher Scientific) followed by biotin-conjugated anti-rabbit IgG Ab. Avidin-peroxidase complex was added and visualized by the addition of 3,3′-Diaminobenzidine chromogenic substrate. Sections were counterstained with hematoxylin, and images were acquired with a Pannoramic 250 Flash II slide scanner (3DHISTEC).

Virus neutralization assay

Generation of an rVSV-expressing enhanced GFP (eGFP) and glycoprotein from EBOV/Mayinga (EBOV/H.sap-tc/COD/76/Yambuku-Mayinga) in place of vesicular stomatitis virus G was described previously (43, 44). Viral neutralization experiments were performed by incubation of titrated amounts of serum from vaccinated mice with a pretitrated amount of rVSV-EBOV (multiplicity of infection ≈ 1 IU per cell) at RT for 1 h prior to addition to Vero cell monolayers cultured in DMEM containing 2% FBS, and 1% penicillin-streptomycin at 37˚C with 5% CO_2. Infection was allowed to proceed for 12–14 h at 37˚C, and viral infectivity was measured by automated counting of eGFP$^+$ cells (IU) using the CellInsight CX5 High-Content Screening Platform (Thermo Fisher Scientific) (41, 43).

Results

Functional subsets of CD4$^+$ T cells induced by BCG vaccination

Studies of T cell responses to BCG vaccination in humans have emphasized mainly the ability of this vaccine to induce CD4$^+$ Th1 cells against secreted bacterial Ags (24–27), although a variety of other defined Th subsets may also be present (26, 29, 45, 46). We used signature markers of well-defined functional Th subsets to more broadly characterize the responses to BCG in a standard mouse model of vaccination. Groups of mice received a single vaccination s.c. of PBS or BCG (1×10^7 CFU), and an additional group received two BCG vaccinations separated by 5 wk (BCG revaccination). Five weeks following the last injection, CD4$^+$ T cells were purified from the spleens of individual mice for ex vivo stimulation with mycobacterial Ags (peptide P25 epitope of Ag85B or *M. tuberculosis* lysate) followed by detection of cytokine secretion by ELISPOT. Sham-vaccinated naive mice (PBS injections) did not develop mycobacteria-specific CD4$^+$ T cell responses to these mycobacterial Ags (data not shown). Similar to BCG vaccination in humans (45, 47, 48), mice in the BCG-vaccinated and -revaccinated groups developed mycobacteria-specific CD4$^+$ T cells with cytokine secretion profiles characteristic of a broad range of Th subsets, including signature cytokines for Th1 (IFN-γ), Th2 (IL-4), Th17 cytokine (IL-17A/F), and Tfh (IL-21) (Fig. 1A). Consistent with this, FACS analysis of CD4$^+$ T cells showed that upon restimulation with mycobacterial Ags, CD4$^+$ T cells from BCG-vaccinated mice expressed the transcriptional regulators Tbet, GATA3, RORγT, and Bcl6, which are associated with the differentiation to individual Th subsets (Fig. 1B; Supplemental Fig. 3A, 3B). Confirming the strong induction of Th1 immunity by BCG (24, 27), intracellular cytokine staining showed higher levels of IFN-γ compared with other cytokines such as IL-21 (Fig. 1C, top). However, these BCG-specific IL-21–secreting CD4$^+$ cells expressed the master transcriptional regulator Bcl6 and the chemokine receptor CXCR5, markers for Tfh (49, 50). These markers were not detected in the CD4$^+$ IFN-γ$^+$ population (Fig. 1C, bottom), suggesting that the majority of IFN-γ–secreting CD4$^+$ T cells were not functionally Tfh.

Design of fusion protein vaccines to capture helper activity of BCG-primed Th cells

The existence of multiple Th subsets specific for mycobacterial Ags following BCG vaccination suggested a general approach that could leverage the helper activity of some of these subsets for Ab production against relevant Ags of other unrelated pathogens. As a proof-of-concept model for the recruitment of BCG-specific Th subsets to promote B cell responses against viral pathogens, we constructed fusion proteins in which either OVA or viral proteins, such as EBOV GP, were fused to immunodominant CD4$^+$ T cell epitopes of mycobacterial Ags Ag85B (P25 epitope) and TB9.8 (P10 epitope). Variants of the fusion proteins were designed with both the P25 and P10 epitopes fused in tandem to the N terminus of the immunogens, designated NTh proteins. Immunogens that only consisted of a single P25 epitope fused to the N terminus were also produced and designated as P25-NTh (Fig. 2A, 2B). These fusion protein vaccines were produced as hexahistidine-tagged soluble proteins, purified by Ni-NTA affinity chromatography and confirmed for correct structure and purity by SDS-PAGE and immunoblotting (Fig. 2C, 2D). To facilitate the proper processing of the BCG epitopes, the endosomal cysteine protease site for CatS was introduced to the flanking region of the individual P25 and P10 epitopes in the NTh version of the EBOV GP (Fig. 2A), OVA fusion protein vaccines, and the single P25 epitope in the P25 NTh version of the OVA fusion protein (Fig. 2B). ELISA was performed with conformational epitope-specific anti–EBOV GP Abs (41) to show that the purified EBOV GP fusion protein vaccine maintained its native structure (Fig. 2E), which is essential for vaccines that require BCR recognition and BCR-mediated Ag uptake.

To demonstrate correct processing and presentation of the MHCII-presented BCG epitopes embedded in the fusion protein vaccines, these were incubated with murine dendritic cells (mDCs) along with Ag85B or TB9.8 TCHs that recognize MHC class II complexed with either P25 or P10 epitopes (51, 52), followed by measurement of IL-2 secretion as an index of T cell Ag-specific responses (Fig. 2F, 2H). The processing and presentation of the P25 epitope flanked by CatS cleavage sites in the P25 NTh OVA fusion protein vaccine was similar to the processing and presentation of the endogenous P25 epitope from the Ag85B protein (Fig. 2G), and these BCG-specific epitopes fused to the fusion protein vaccine of EBOV (Fig. 2F) or OVA (Fig. 2H) were all efficiently processed by dendritic cells and presented to T cells in vitro.

Enhanced Ab responses to fusion proteins in BCG-primed mice

For initial studies, fusion protein vaccines constructed with OVA linked to BCG Th epitopes were administered into mice as a mixture with alum to provide an Ag depot and adjuvant effects. To reveal the contribution of BCG priming in promoting Ab responses, the dose for the fusion protein vaccine was titrated from 1 to 0.01 μg per mouse. In mice that were primed only with PBS injections and lacked BCG-specific Th cells, fusion protein–specific IgG Abs were induced only at the highest doses (1–0.1 μg), whereas a lower dose (0.01 μg) yielded an undetectable Ab titer. In contrast, mice that had been previously primed with BCG had readily detectable Ab responses to the fusion protein vaccine at the dose of 0.01 μg (Fig. 3A). Analysis of Ab isotype showed that significant class switching to IgG2c occurred only in the BCG-primed mice and not in PBS-primed mice even after administration of high doses (1–0.1 μg) of the fusion protein vaccine (Fig. 3B). To assess memory B cell formation induced by the initial fusion protein vaccine, a second homologous boost with the same dose (0.01 μg)
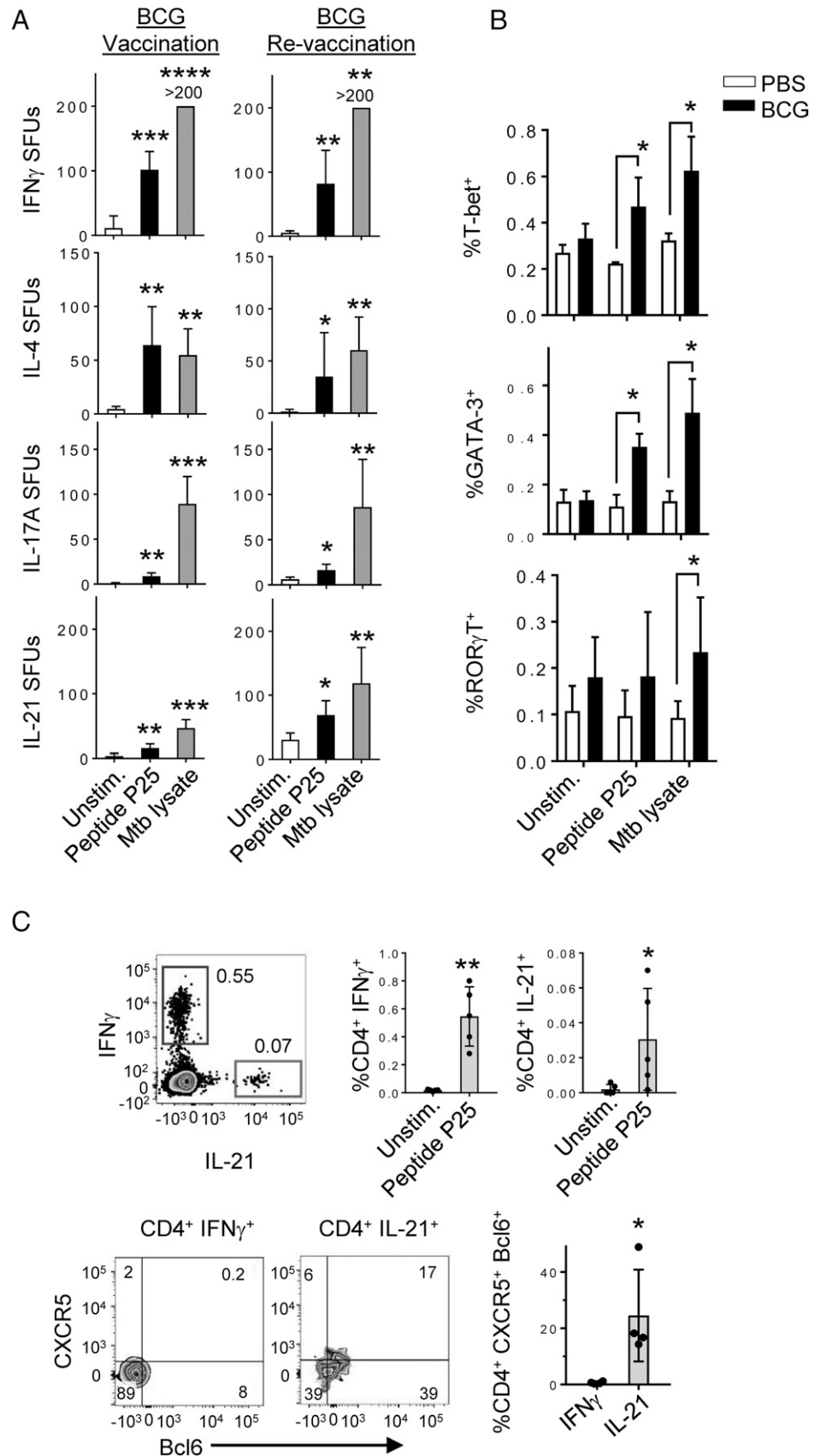
FIGURE 1. BCG vaccination induces a broad range of Th subsets. (A) ELISPOT of purified CD4$^+$ T cells from BCG-vaccinated and BCG-revaccinated mice and (B) FACS analysis on splenocytes from BCG-vaccinated mice were performed to detect signature cytokines and transcriptional makers that corresponds to distinct subsets of Th cells after restimulation ex vivo with BCG Ags in the form of peptide or bacterial lysate. Mean $\pm$ SD for five replicates is shown, and data are representative of three separate experiments. $*p < 0.05$, $**p < 0.01$, $***p < 0.001$, $****p < 0.0001$, Kruskal–Wallis one-way ANOVA, with post hoc analysis using the Mann–Whitney U test with Bonferroni correction to adjust the probability. (C) FACS analysis on splenocytes from BCG-vaccinated mice that were gated on CD4$^+$ T cells detected IFN-γ and IL-21 secretion upon restimulation with peptide P25 (top). Tfh markers CXCR5 and Bcl6 were only detected in IL-21–secreting CD4$^+$ T cells (bottom). Mean $\pm$ SD for five replicates is shown, and data are representative of three separate experiments. $*p < 0.05$ $**p < 0.01$, Mann–Whitney t test used to comparing between the two columns.

of the fusion protein vaccine was administered. The PBS-primed mice that lacked BCG-specific Th cells and produced undetectable IgG Ab titers to the initial 0.01 µg per mouse vaccine dose responded to the second homologous boost with total IgG Ab titers similar to those of BCG-primed mice that received the same vaccination regimen (Fig. 3C). However, the second homologous boost was still unable to induce IgG2c class switching in PBS-primed mice as compared with BCG prime mice (Fig. 3D), indicating a
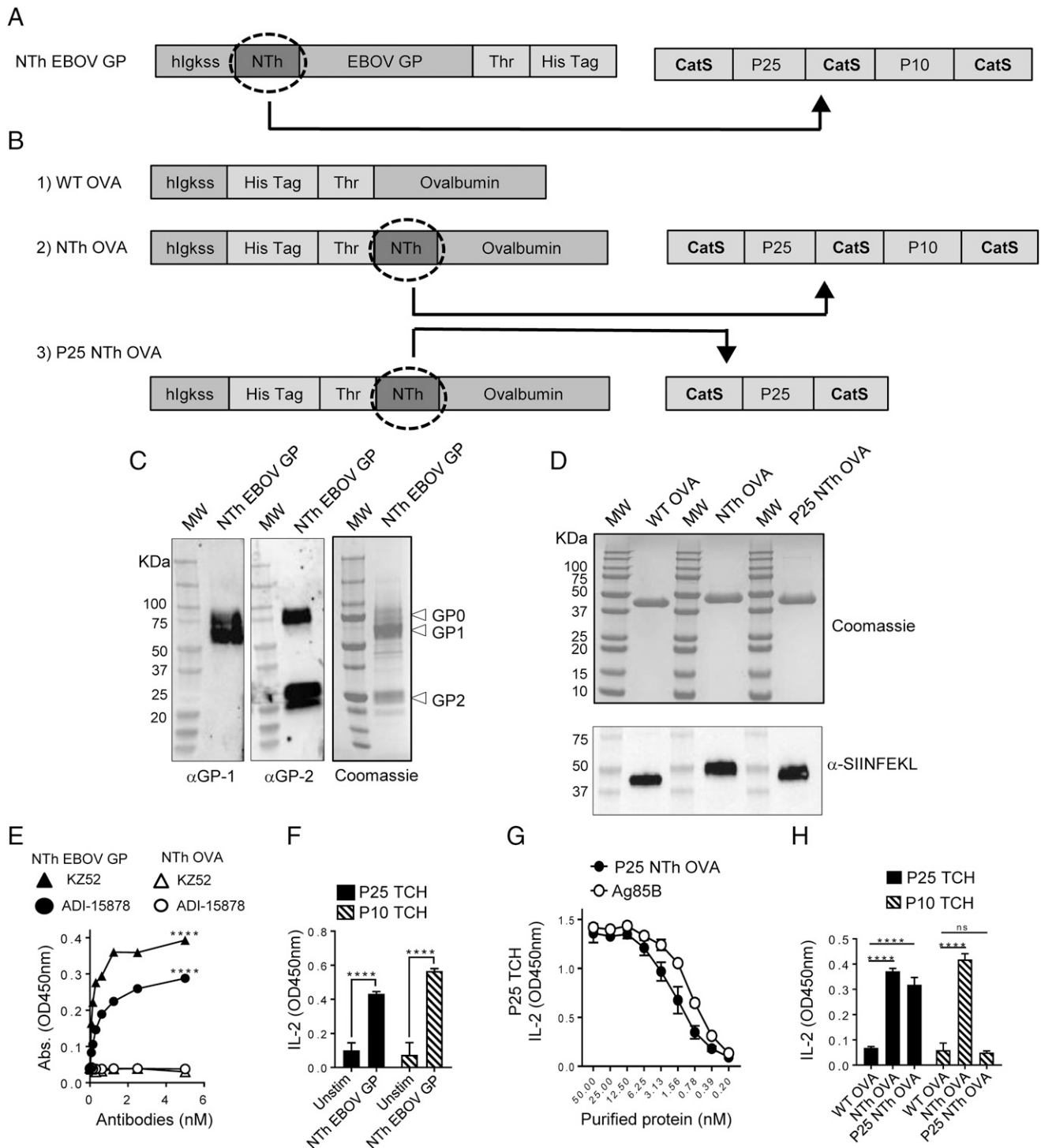
FIGURE 2. Purification and characterization of fusion protein vaccine constructs. Schematic design of (**A**) the EBOV GP and (**B**) OVA fusion protein vaccine constructs (hIgss, Thr, and CatS). SDS-PAGE analysis of purified (**C**) EBOV GP and (**D**) OVA fusion protein vaccines as shown by Coomassie Blue staining and immunoblotting with anti–EBOV GP or anti-SIINFEKL Abs. (**E**) Anti-EBOV GP Abs (ADI-15878 and KZ52) that recognize conformational epitopes were used in ELISA to detect proper folding of glycoprotein in the fusion protein vaccine. ****$p < 0.0001$, two-way ANOVA followed by a Tukey multiple comparisons test to evaluate significance between groups. (**G**) CatS engineered to flank the P25 epitope in the fusion protein vaccine showed similar efficiency as compared with the endogenous P25 from the purified Ag85B protein for processing and presentation of the P25 peptide by dendritic cells, as detected by ELISA for the release of IL-2 from P25-specific TCH. (**F–H**) The proper processing and presentation of BCG-specific epitopes by dendritic cells after uptake of (F) EBOV GP or (H) OVA versions of the fusion protein vaccine were detected by P25 and P10 TCHs specific for BCG epitopes in Ag85B and TB9.8, respectively. Activation of TCH is measured by ELISA for IL-2 released into the supernatant. Mean $\pm$ SD for six replicates is shown, and data are representative of two independent experiments. ****$p < 0.0001$, two-way ANOVA followed by a Sidak or Dunnett multiple comparisons test to evaluate the significance between groups. CatS, cathepsin cleavage site; hIgss, human Ig κ signal sequence; Thr, thrombin cleavage sites.
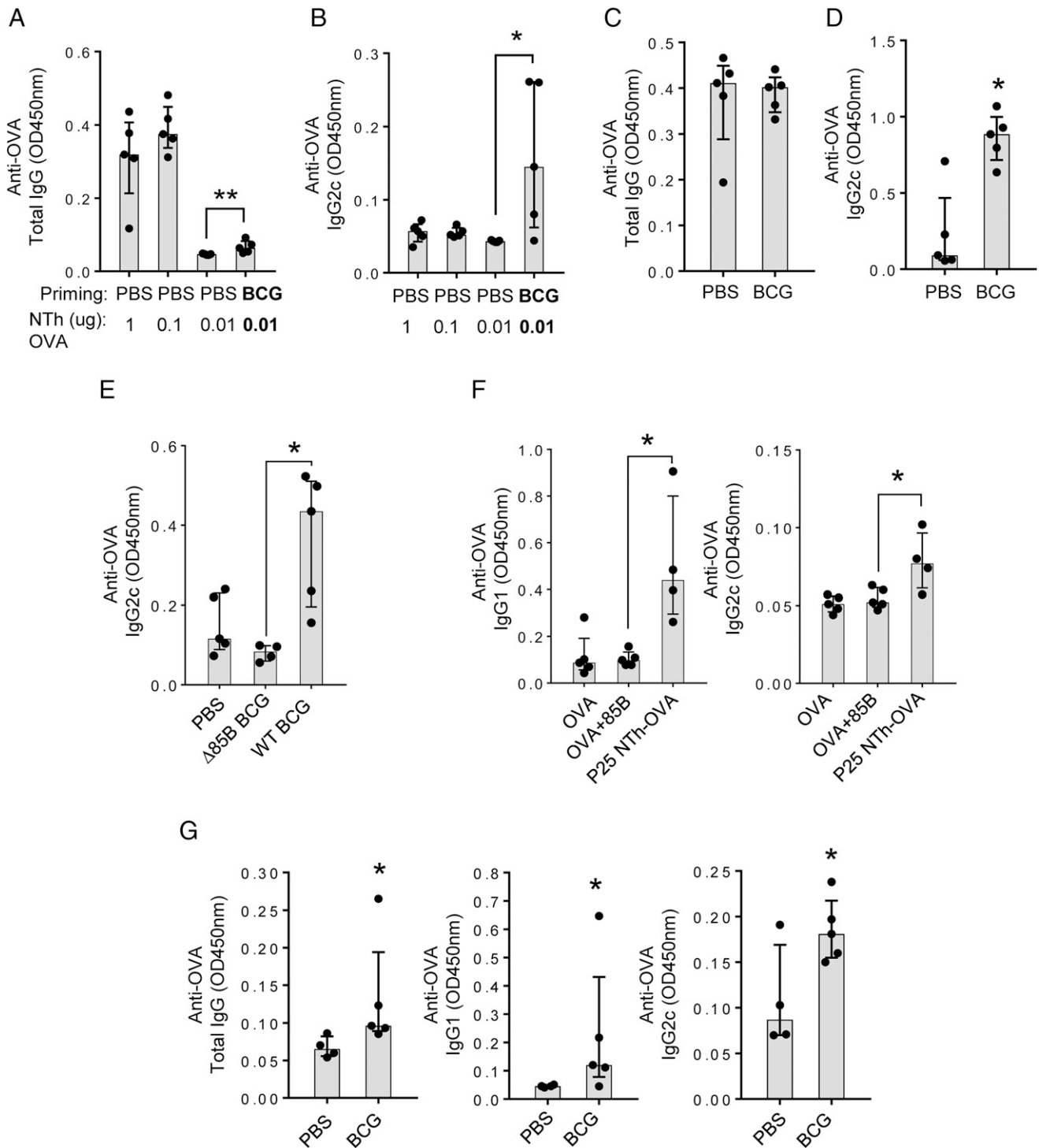
FIGURE 3. BCG-specific CD4^{+} T cells and linked recognition are required to provide dose-sparing effect of the fusion protein vaccine and drive class-switching Ab responses. (**A** and **B**) PBS- or BCG-primed mice were boosted with indicated dose of OVA fusion protein vaccine (NTh OVA) ranging from 1 to 0.01 μg per mouse, and sera were analyzed for OVA-specific (A) total IgG and (B) IgG2c. (**C** and **D**) After 4 wk, a second boost with 0.01 μg of OVA fusion protein vaccine (NTh) were given to mice that initially received the 0.01 μg dose of the OVA fusion protein vaccine. Sera were analyzed for OVA-specific (C) total IgG and (D) IgG2c. (**E**) Mice vaccinated with PBS, WT, or Δ85B BCG were boosted with the OVA fusion protein vaccine (P25-NTh), and sera were collected and analyzed for OVA-specific IgG2c. (**F**) BCG-vaccinated mice were boosted with WT OVA, OVA with Ag85B protein (85B), or the OVA fusion protein vaccine (P25-NTh OVA), and sera were collected and analyzed for OVA-specific IgG1 and IgG2c. (**G**) Six months after BCG vaccination, mice were boosted with the NTh OVA fusion protein vaccine, and sera were analyzed 2 wk later by ELISA for Ag-specific Abs. Median with interquartile range for at least four replicates are shown. A Mann–Whitney U test was used for pairwise comparisons, and a Kruskal–Wallis one-way ANOVA test for multiple comparisons. For post hoc analysis after Kruskal–Wallis test, a Mann–Whitney U test using the Bonferroni correction was used to adjust for significance between groups. $*p < 0.05$, $**p < 0.01$.

requirement for BCG-specific Th cells to induce class switching to this isotype.

*Requirement for linked recognition for BCG enhancement of Ab responses*

We used a BCG mutant lacking expression of Ag85B (Δ85B) to assess the requirement for specific mycobacterial Ag recognition and direct linkage of this to the Ab target of the P25-NTh OVA fusion protein. The Δ85B BCG mutant was created through allelic exchange to delete the *fpbp* gene encoding Ag85B (Supplemental Fig. 1A, 1B). The expression of Ag85B was determined by the activation of a P25-specific TCH, which was activated by mDCs infected with the WT BCG but not the ΔAg85 mutant BCG (Supplemental Fig. 1C; top). A TCH specific for BCG isocitrate lyase (53) served as a control to confirm similar levels of infection of mDCs with the WT and mutant BCG (Supplemental Fig. 1C; bottom). To confirm that vaccination with the ΔAg85B mutant BCG did not elicit P25-specific CD4^{+} T cells, splenocytes from mice vaccinated with WT, Δ85B, or Δ85B BCG complemented with *fbpb* were restimulated in vitro with the P25 peptide or *M. tuberculosis* lysate, and the release of IFN-γ into culture supernatants was assayed by capture ELISA. Stimulation with *M. tuberculosis* lysate showed that all three BCG vaccine strains (WT, Δ85B, and 85B complemented) induced similar Th cell responses toward mycobacterial lysate. P25-specific Th cells were induced, as shown by restimulation of splenocytes with P25 peptide, in mice vaccinated with either the WT or the 85B-complemented

BCG strains but not in the Δ85B BCG mutant–vaccinated mice that had similar Th responses as those in the unstimulated groups (Supplemental Fig. 1D), which were comparable to naive mice (data not shown) (54).

To test whether P25-specific CD4^{+} T cells were required to induce Ab responses to the fusion protein vaccine, mice were primed with PBS, WT, or Δ85B BCG followed by vaccination with the P25-NTh OVA fusion protein vaccine. Mice primed with WT BCG promoted IgG2c Abs specific for OVA, whereas animals primed with Δ85B BCG did not (Fig. 3E). The classic mechanism of linked recognition in specific Th interactions with B cells requires that the T cell epitope must be tightly associated, generally by a covalent bond, with the immunogen that is recognized by the cognate BCR (55). Consistent with this principle, in BCG-vaccinated mice that developed P25-specific Th cells, administering the OVA immunogen that lacked the P25 epitope (WT OVA) or WT OVA in a mixture together with the Ag85B protein (WT OVA plus 85B) failed to promote OVA-specific Abs (Fig. 3F). This confirmed the requirement for covalent linkage of the P25-specific CD4^{+} T cell epitope to the OVA immunogen for recruitment of BCG-induced Th activity and indicated that the effects on Ab responses of BCG-primed animals were unlikely to be due to the prolonged trained innate immunity effects that can follow BCG vaccination (56, 57).

BCG vaccination is most commonly given to neonates, leading to BCG-specific memory Th cells that persist at least into young adulthood and are frequently boosted by subsequent exposure to

FIGURE 4. BCG-specific Th cells promote neutralizing anti–EBOV GP Abs following vaccination with EBOV GP fusion protein vaccine. (**A**) Anti–EBOV GP IgG1 and IgG2 Ab titer measured by ELISA from sera in PBS- and BCG-primed mice (n = 4) after administering NTh EBOV GP fusion protein vaccine. (**B** and **C**) Sera from naive (n = 1), PBS- (n = 10), or BCG- (n = 10) primed mice vaccinated with NTh EBOV GP fusion protein vaccine were incubated with rVSV–EBOV GP–expressing GFP to determine the neutralization capacity of anti–EBOV GP Abs to prevent entry into Vero cells, as shown by (B) representative microscopy images (original magnification ×40) and by (C) IC$_{50}$ quantification. Experiments were repeated twice. *p < 0.05, **p < 0.01, Mann–Whitney *U* test for pairwise comparison.
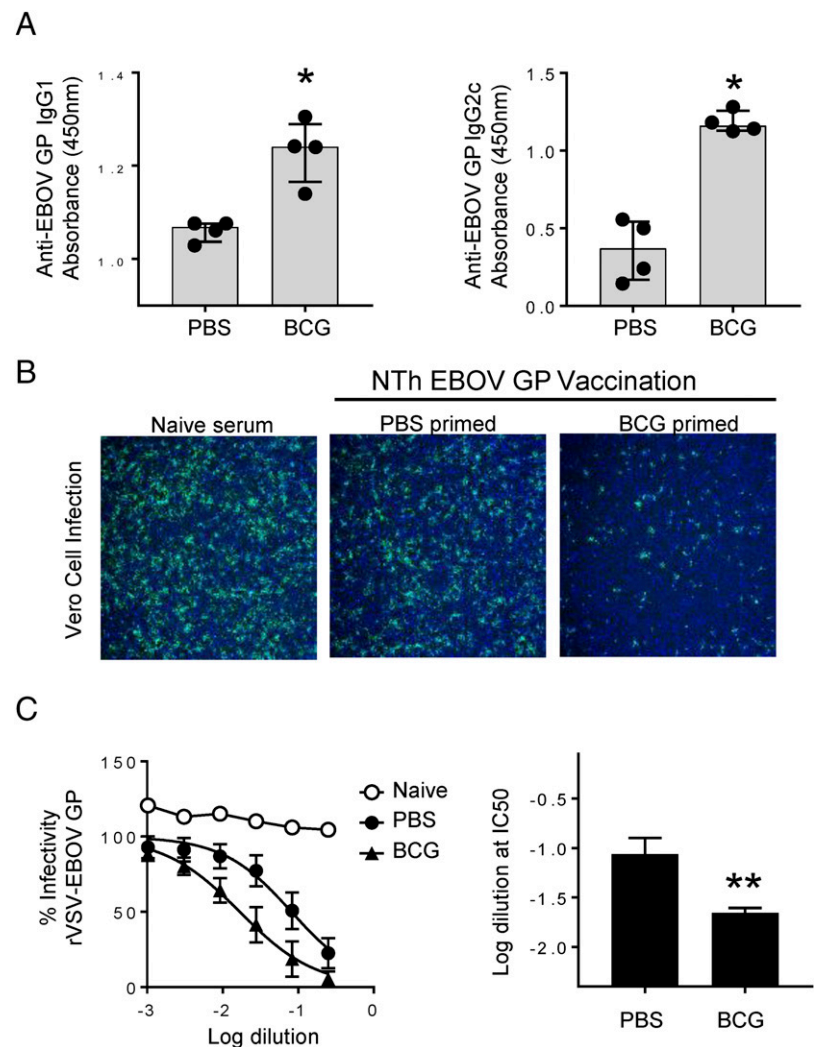
M. tuberculosis or nontuberculous mycobacteria (58). To more accurately model this situation in mice, we expanded the time interval between BCG priming and vaccination with the fusion protein vaccine by resting the animals for 6 mo after priming before vaccinating with the fusion protein vaccine. These animals continued to show enhancement of Ab production with BCG priming, indicating that the relevant BCG-specific memory Th cells were sufficiently long-lived to provide the dose-sparing and isotype-switching effects even without subsequent boosting with mycobacterial Ags (Fig. 3G). This result also suggested that the observed effects of BCG priming in this model were likely to depend on long-lived memory T cells and not on the more transient effects of BCG on trained innate immunity (56, 57).

Increased antiviral activity, avidity, and persistence of Abs induced by BCG-specific Th cells

To study the potential for Abs driven by BCG-specific Th cells to neutralize viral entry and infection, we employed a standard model for assaying effects on EBOV entry (41). PBS or BCG-primed mice were vaccinated with 0.01 μg of the EBOV GP fusion protein vaccine (NTh EBOV GP) per mouse, and 2 wk later sera were analyzed for anti–EBOV GP–specific IgG1 and IgG2c (Fig. 4A). A second boost with the same dose of the EBOV fusion protein vaccine was administered 10 wk later, and sera were collected for viral neutralization assay, in which an EBOV GP pseudotyped rVSV (rVSV-EBOV GP) expressing GFP was used to measure EBOV GP–mediated entry of the virus into Vero cells (Fig. 4B). This revealed significantly improved neutralization of viral entry with sera from the BCG-primed group as compared with the PBS-primed group (Fig. 4C), consistent with either increased Ab concentration or avidity or both in the BCG-primed group.

Neutralizing Abs are often developed from B cell clones that undergo affinity maturation through multiple rounds of mutation and selection in GCs reactions, resulting in Abs with increased avidity toward their Ags. To determine which subclasses of IgG developed into high-avidity Abs, BCG-primed mice were vaccinated twice with the fusion protein vaccine NTh OVA at 4-wk intervals. Serum samples were incubated with OVA-coated ELISA

wells to allow for Ab–Ag interactions, and avidity of the anti-OVA Abs was measured by their ability to resist elution by GuHCl, a chaotropic agent used to disassociate Ab–Ag interactions (42). Anti-mouse IgG1 or IgG2c Abs were used to probe for the subclass of mouse anti-OVA Abs that remained bound to OVA. Both IgG1 and IgG2c binding was sensitive to GuHCl elution after the first NTh OVA boost. However, after the second NTh OVA boost, the IgG1 anti-OVA Abs became significantly more resistant to GuHCl elution, whereas IgG2c Abs remained susceptible to GuHCl disruption of binding (Fig. 5A). This suggested that the IgG1 subclass of anti-OVA Abs underwent maturation with repeated boosting into higher-avidity Abs, consistent with multiple rounds of mutation and selection in GCs. In contrast, IgG2c anti-OVA Abs did not show this affinity maturation, suggesting that they may be primarily produced by B cells located outside of GCs.

We also assessed the kinetics of anti-OVA Ab titers that developed in BCG-primed mice after each NTh OVA boost by obtaining serum samples at 1, 2, 3, and 8 wk after the first NTh OVA boost, and at 2 and 8 wk after the second NTh OVA boost (Fig. 5B). Both the IgG1 and IgG2c subclasses of anti-OVA Ab responses peaked at week 2 following the first NTh OVA boost and then diminished significantly by 8 wk. Administering a second NTh OVA boost increased the titers of both anti-OVA IgG1 and IgG2c subclasses to levels that surpassed the first vaccination. These Ab titers were increased and remained elevated for a prolonged period after the second boost, suggesting the formation of memory B cells and long-lived plasma cells.

Localization of BCG-specific Th cells in secondary lymphoid tissue

GCs are discrete structures within the B cell follicles, where B cells undergo somatic hypermutation and affinity maturation. Sustaining the GCs reaction requires Tfh, a particular Th subset that localizes predominantly to the light zone of the GC (59). To directly visualize the location of BCG-specific Th cells within a secondary lymphoid organ, adoptive cell transfer was performed in which GFP+ P25 Tg TCR CD4+ T cells were transferred into

FIGURE 5. Development of high-affinity IgG1 subclass and kinetics of fusion protein vaccine-specific Ab responses. (**A**) BCG-primed mice (*n* = 8) were boosted twice with the NTh OVA fusion protein vaccine, and serum samples were collected and stored at −80°C after each fusion protein vaccine boost for future analysis. A modified ELISA that consists of a GuHCl treatment step was used to analyze the serum for measuring Ab affinity. Experiments were repeated twice. **p < 0.01, ***p < 0.001, Mann–Whitney *U* test used for pairwise comparisons. (**B**) BCG-primed mice (*n* = 5) were boosted with the OVA fusion protein vaccine, and sera were collected at week 1, 2, 3, and 8 and stored at −80°C for future analysis. Mice were then boosted again with OVA fusion protein vaccine, and sera were collected at week 2 and 8. All sera were assayed by ELISA for Ag-specific IgG1 and IgG2c Abs. Experiment was done once. *p < 0.05, Kruskal–Wallis one-way ANOVA with post hoc analysis using the Mann–Whitney *U* test with Bonferroni correction to adjust the probability.
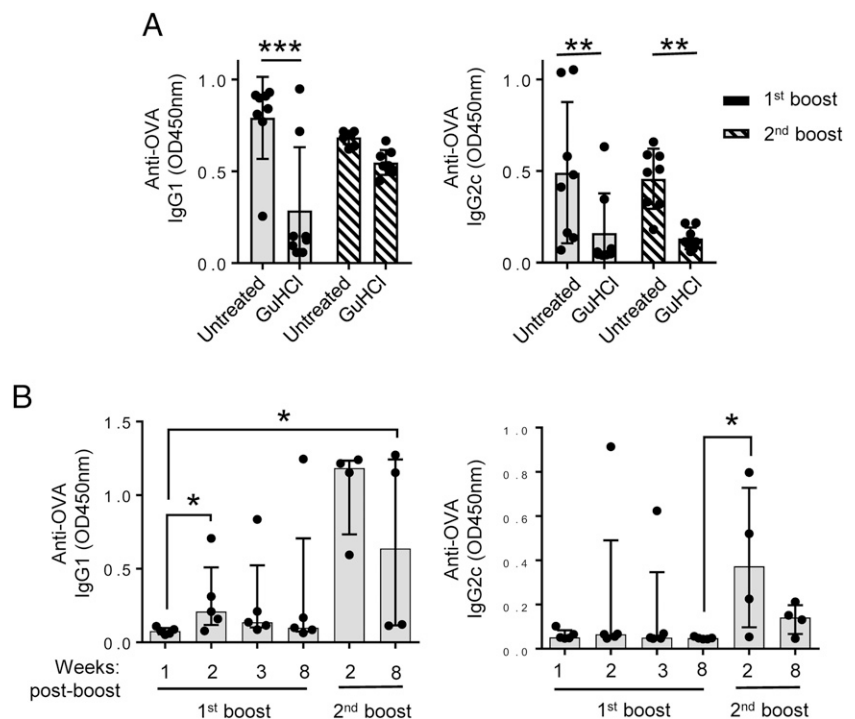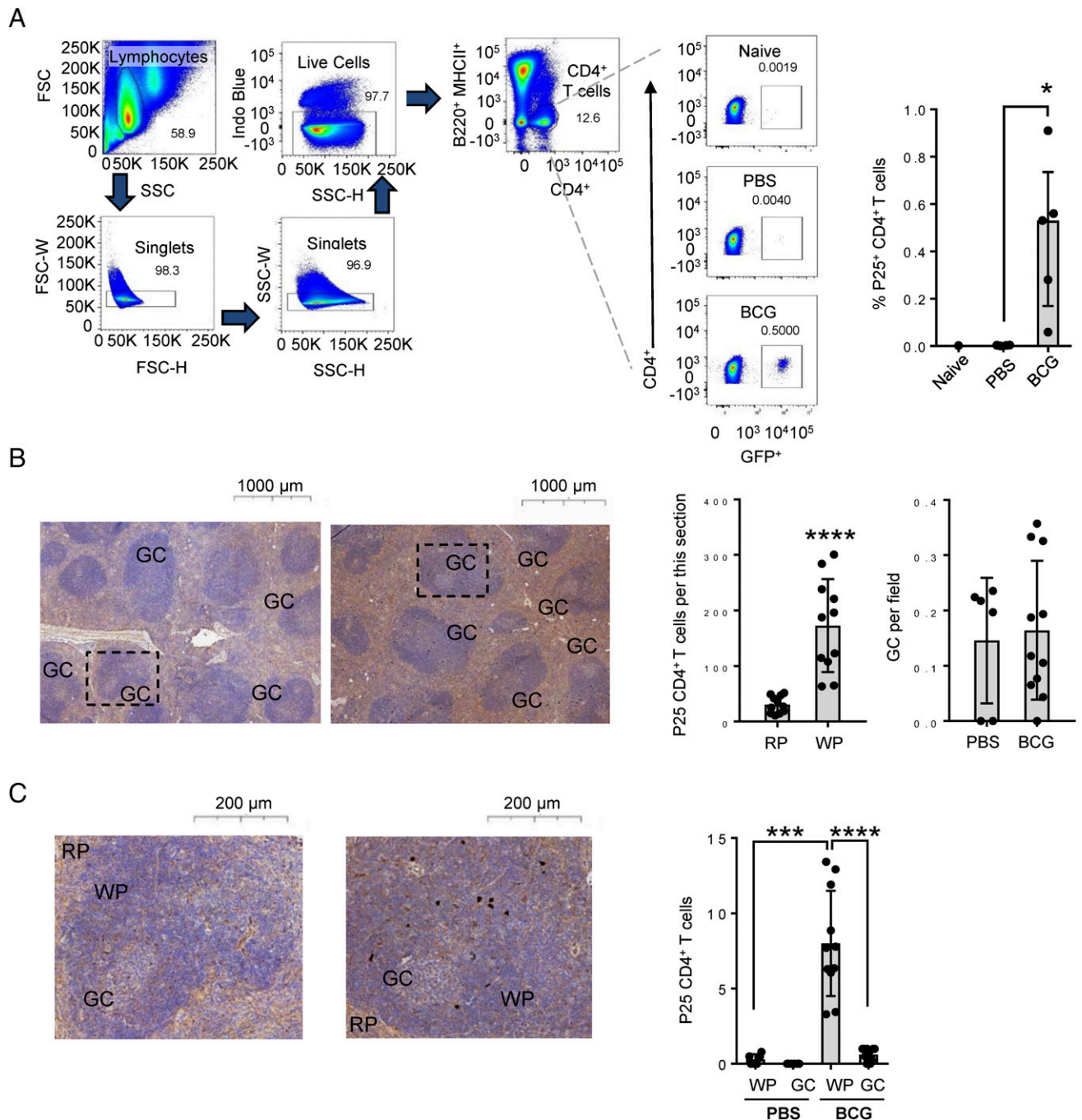
FIGURE 6. Localization of P25-specific T cells in the spleen. Mice ($n = 5$) were adoptively transferred with 4×10^4 CD4^{+} T cells purified from P25 TCR-Tg GFP^{+} mice 16 h prior to vaccination with PBS or BCG. The animals were sacrificed 6 d after vaccination, and spleens were bisected for (A) processing into splenocytes for FACS analysis and (B and C) fixation for histology. (A) Gating strategy to isolate lymphocytes, followed by gating on singlets. Dead cells and B220^{+} MHCII^{+} cells were excluded from the analysis. Total CD4^{+} T cells were gated followed by GFP^{+} signal to detect the adoptively transferred P25 TCR-Tg cells. (B and C) Formalin-fixed and paraffin-embedded spleens were cut into thin sections for immunocytochemistry with anti-GFP followed and counterstained with hematoxylin. White pulp (WP), red pulp (RP), and GCs were quantified. Experiment was performed once. *$p < 0.05$, ****$p < 0.0001$, Mann–Whitney U test for pairwise comparison; ***$p < 0.001$, ****$p < 0.0001$ for multiple columns, Kruskal–Wallis one-way ANOVA followed by Dunnett multiple comparisons test to evaluate the significance.

mice 16 h before priming with PBS or BCG. Spleens were harvested 6 d later for analyses by FACS (Fig. 6A) and immunohisto-chemistry (Fig. 6B, 6C). FACS analysis showed that the transferred GFP^{+} P25 Tg TCR CD4^{+} T cells expanded following BCG priming (Fig. 6A), and these GFP^{+} cells were predominantly localized to the white pulp and not the red pulp of the spleen (Fig. 6B). Although the numbers of GCs were similar between PBS and BCG-primed groups (Fig. 6B), there were more GFP[+]

cells in the BCG-primed group, with the majority of these GFP^{+} cells in the extrafollicular areas and away from GCs (Fig. 6C).

Assessment of Th priming with neonatal BCG vaccination and adult revaccination

In countries with a high prevalence of *M. tuberculosis* infection, the BCG vaccine is routinely administered to most infants shortly after birth. BCG vaccine given to neonates induces BCG-specific
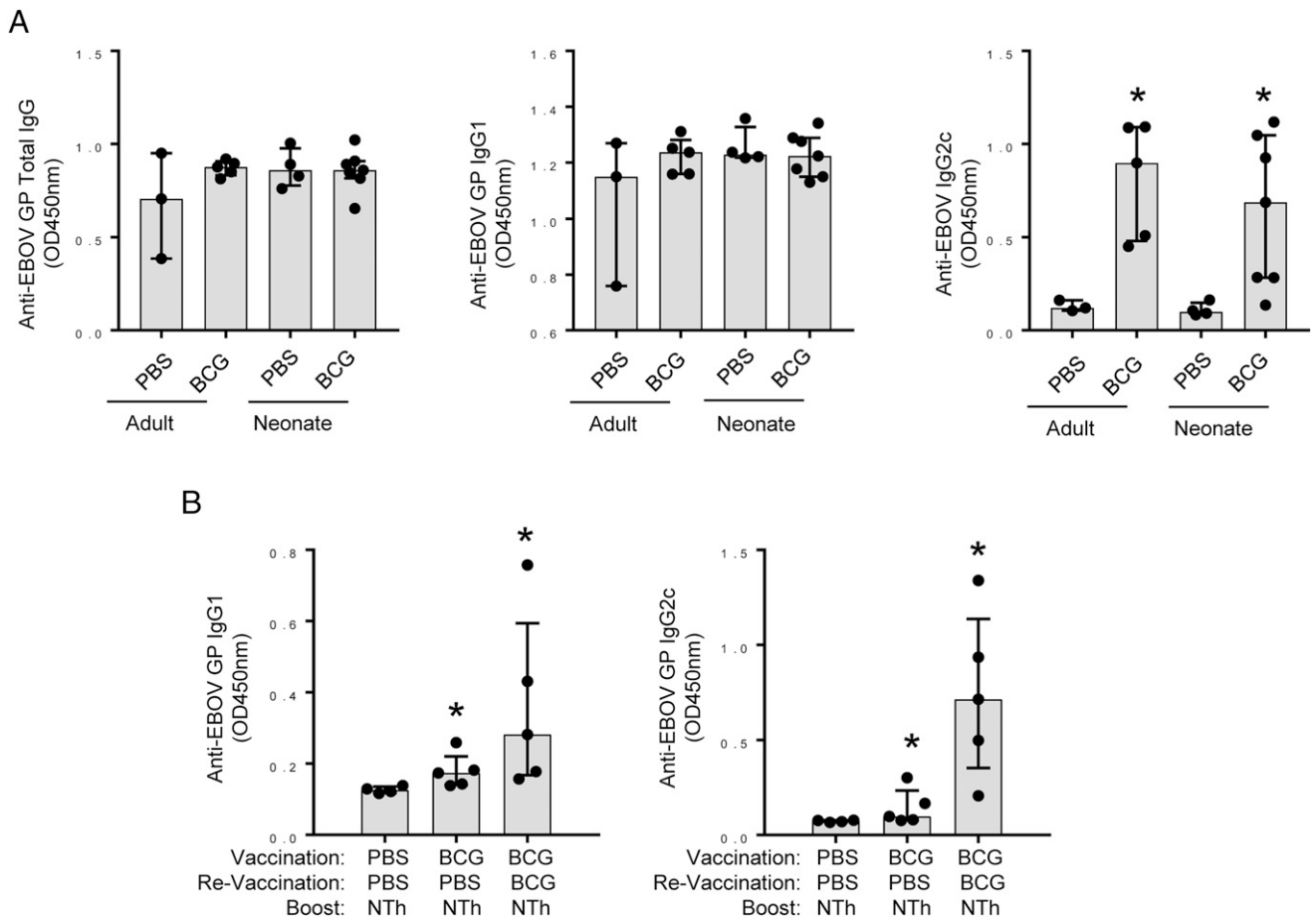
FIGURE 7. Assessment of fusion protein vaccine in neonatal BCG vaccination and adult BCG revaccination. (**A**) Five-week-old adult or five-day-old neonate mice ($n = 3$–7) were primed with PBS or BCG, followed by vaccination with the NTh EBOV GP fusion protein vaccine. Sera were collected and analyzed by ELISA for Ag-specific IgG1 and IgG2c Abs. (**B**) Mice were vaccinated with PBS ($n = 4$), BCG ($n = 5$), or revaccinated with BCG ($n = 5$), followed by administering the NTh EBOV GP fusion protein vaccine. Sera were analyzed by ELISA for Ag-specific IgG1 and IgG2c Abs. *$p < 0.05$, Kruskal–Wallis one-way ANOVA with post hoc analysis using the Mann–Whitney U test with Bonferroni correction to adjust the probability.

Th subsets that may differ functionally from those that develop in subjects receiving BCG vaccination later in life (60), and these differences could have an impact on responses to fusion protein vaccines that recruit BCG-specific Th cells. To test this, BCG was administered to 5-d-old and 5-wk-old mice that were then rested for 5 wk before administering the NTh EBOV GP fusion protein vaccine. Mice that received neonatal BCG vaccination at 5 d of age showed similar Ab responses to EBOV GP compared with those that received adult BCG vaccination at 5 wk, especially in the induction of IgG2c (Fig. 7A).

A recent clinical study has suggested beneficial effects of BCG revaccination in adults for enhancing anti–*M. tuberculosis* immunity (61), and this has generated renewed interest in applying such revaccination to future vaccine regimens against tuberculosis. To explore the impact of BCG revaccination on the enhancement of Ab responses against the NTh EBOV GP fusion protein in our mouse model, mice were primed once with PBS or BCG, or primed with BCG and revaccinated 6 wk later with BCG before administering the fusion protein vaccine (Fig. 7B). As seen before, the presence of BCG-specific Th cells in BCG-primed mice promoted higher Ab titers to the fusion protein vaccine as compared with PBS-primed mice that lacked BCG-specific Th cells (Figs. 3, 4A, 7B). In BCG-revaccinated mice, a further increase of Ab titers to the fusion protein in both IgG1 and IgG2c subclasses was observed as compared with mice that were primed only once with BCG (Fig. 7B, Supplemental Fig. 4). These results indicated a

potential advantage from BCG revaccination in reinforcing and augmenting the BCG-specific Th activity for Ab responses to the fusion protein immunogen.

Discussion

The concept of linked recognition in T cell–dependent generation of Ab responses is well established and is the basis of many effective conjugate vaccines (9, 11, 12, 62). In the current study, we adopted this basic principle by using covalently linked BCG Th epitopes in fusion protein immunogens to enhance vaccination for stimulation of Ab responses. Our approach was largely motivated by the fact that there is a large human population with pre-existing BCG-specific Th cells acquired during BCG vaccination at birth. Our results showed that BCG vaccination induces a broad spectrum of Th cells that can be recruited by the BCG CD4$^+$ T cell epitope on the fusion protein vaccine to promote the development of Abs that are likely to be protective if directed against relevant targets such as viral surface glycoproteins. Abs produced with recruitment of BCG-specific Th cells included high-affinity neutralizing IgG Abs as well as ADCC promoting Abs of the IgG2 subclass. Both of these are known to be important for protection against viral pathogens, as shown in mouse models of viral infections such as influenza (14).

The administration of our fusion protein vaccines following BCG priming consistently induced IgG2c class-switched Abs with lower affinity as compared with their IgG1 counterparts (Fig. 5A).

These low-affinity IgG2c Abs most likely developed from extra-follicular sites outside of the GC. Indeed, as shown in our adoptive transfer experiments using P25 GFP⁺ cells, most of BCG-specific T cells localized outside of the GC (Fig. 6C), suggesting that their extrafollicular positioning and, subsequently, the location for B cell interaction outside the GCs resulted in the production of relatively low-affinity Abs. Furthermore, the entry of Th cells into the GCs requires chemokine receptors, such as CXCR5, which were absent from the majority of IFN-γ–secreting CD4⁺ T cells in the BCG-vaccinated mice (Fig. 1C), providing further support that these BCG-specific Th1 cells contributed to the promotion of IgG2c Abs that developed in extrafollicular foci without under-going affinity maturation in the GCs.

Our results also showed that recruitment of BCG-specific Th cells using the fusion protein approach also gave a significant dose-sparing effect for the induction of IgG1 Ab responses when compared directly to vaccination with alum-adjuvanted protein in BCG naive animals. This most likely was due to the fact that BCG priming also induced a population of Th cells with the typical features of conventional Tfh, including the production of cy-tokines important for B cell differentiation and maturation of Ab responses such as IL-4 and IL-21. Because of increased affinity, these Ag-specific IgG1 Abs induced by BCG-specific Tfh most likely developed in GCs and conferred neutralizing capabilities that prevented viral infection in our model system for EBOV infection (Fig. 4B). Although, BCG priming provided a dose-sparing effect on the recombinant fusion vaccine in the devel-opment of these neutralizing IgG1 Abs, the subtle increase in IgG1 can easily be obscured by a slight increase in vaccine dose, especially with alum as an adjuvant, which also promotes IgG1 responses (Fig. 7A). The contribution of BCG-specific Tfh to promoting high-affinity neutralizing IgG1 Ab responses could be significantly enhanced in mice that received BCG vaccina-tion twice before administering the fusion protein vaccine (Fig. 7B, Supplemental Fig. 4). Recent clinical studies have indicated that BCG revaccination may improve protection against *M. tuberculosis* (61), which may lead to the frequent use of such regimens in re-gions with a high prevalence of tuberculosis. If so, the quality of BCG-specific Th cells resulting from BCG revaccination could further enhance the Ab responses generated using our fusion protein vaccines.

Our work demonstrates that the pre-existing BCG-specific Th cells, including Th1 and Tfh, contribute to the development of IgG1 and IgG2c Abs elicited by fusion protein vaccines engineered to recruit the activities of these Th cells. Although our studies in the mouse model showed that a majority of BCG-specific Th cells are extrafollicular Th1 cells that promote low-affinity IgG2c Ab re-sponses, we also demonstrated a small population of BCG-specific Tfh that drives the development of high-affinity IgG1 Abs. By modulating the BCG-specific Th subsets, such as in BCG revac-cination or by modifying BCG, it may be possible to adjust the balance of Th subsets to further optimize the levels of neutralizing and ADCC-promoting Abs. In our studies to assess vaccine design involving recruitment of pre-existing BCG-induced Th cell Ab responses, comparisons with immunization using alum as an ad-juvant were used because of the well-established use of this ad-juvant with purified protein vaccines. It is possible that other chemical adjuvants could generate responses similar to those ob-tained with our approach without requiring BCG priming and linked recognition of the immunogen, Thus, our vaccination ap-proach is by no means a replacement for the use of other more powerful adjuvants that are entering clinical use, such as MF59, which has been shown to promote many of the advantages we observed with BCG priming (63, 64), and may in some cases bypass

the need for Th cell priming (65). However, given the continued widespread use of BCG vaccination in many of the regions that are most frequently afflicted by emerging viral pathogens, our approach may be useful as a safe and cost-effective component of vaccination regimens to rapidly contain initial outbreaks of disease.

Disclosures

The authors have no financial conflicts of interest.

References

1. World Health Organization. Emergencies preparedness, response. Available at: https://www.who.int/csr/don/archive/year/2019/en/. Accessed: October 31, 2019.
2. Grubaugh, N. D., J. T. Ladner, P. Lemey, O. G. Pybus, A. Rambaut, E. C. Holmes, and K. G. Andersen. 2019. Tracking virus outbreaks in the twenty-first century. *Nat. Microbiol.* 4: 10–19.
3. Bornholdt, Z. A., H. L. Turner, C. D. Murin, W. Li, D. Sok, C. A. Souders, A. E. Piper, A. Goff, J. D. Shamblin, S. E. Wollen, et al. 2016. Isolation of potent neutralizing antibodies from a survivor of the 2014 Ebola virus outbreak. *Science* 351: 1078–1083.
4. Karasavvas, N., E. Billings, M. Rao, C. Williams, S. Zolla-Pazner, R. T. Bailer, R. A. Koup, S. Madnote, D. Arworn, X. Shen, et al; MOPH TAVEG Collabo-ration. 2012. The Thai phase III HIV type 1 vaccine trial (RV144) regimen in-duces antibodies that target conserved regions within the V2 loop of gp120. *AIDS Res. Hum. Retroviruses* 28: 1444–1457.
5. Rimoin, A. W., K. Lu, M. S. Bramble, I. Steffen, R. H. Doshi, N. A. Hoff, P. Mukadi, B. P. Nicholson, V. H. Alfonso, G. Olinger, et al. 2018. Ebola virus neutralizing antibodies detectable in survivors of theYambuku, Zaire outbreak 40 years after infection. *J. Infect. Dis.* 217: 223–231.
6. Kim, J. H., J. L. Excler, and N. L. Michael. 2015. Lessons from the RV144 Thai phase III HIV-1 vaccine trial and the search for correlates of protection. *Annu. Rev. Med.* 66: 423–437.
7. Watts, C. 1997. Capture and processing of exogenous antigens for presentation on MHC molecules. *Annu. Rev. Immunol.* 15: 821–850.
8. Cherukuri, A., P. C. Cheng, and S. K. Pierce. 2001. The role of the CD19/CD21 complex in B cell processing and presentation of complement-tagged antigens. *J. Immunol.* 167: 163–172.
9. Parker, D. C. 2013. The carrier effect and T cell/B cell cooperation in the an-tibody response. *J. Immunol.* 191: 2025–2027.
10. Goldblatt, D. 2000. Conjugate vaccines. *Clin. Exp. Immunol.* 119: 1–3.
11. Pichichero, M. E. 2013. Protein carriers of conjugate vaccines: characteristics, development, and clinical trials. *Hum. Vaccin. Immunother.* 9: 2505–2523.
12. Fraser, C. C., D. H. Altreuter, P. Ilyinskii, L. Pittet, R. A. LaMothe, M. Keegan, L. Johnston, and T. K. Kishimoto. 2014. Generation of a universal CD4 memory T cell recall peptide effective in humans, mice and non-human primates. *Vaccine* 32: 2896–2903.
13. Zeltins, A., J. West, F. Zabel, A. El Turabi, I. Balke, S. Haas, M. Maudrich, F. Storni, P. Engeroff, G. T. Jennings, et al. 2017. Incorporation of tetanus-epitope into virus-like particles achieves vaccine responses even in older re-cipients in models of psoriasis, Alzheimer's and cat allergy. *NPJ Vaccines* 2: 30.
14. Miyauchi, K., A. Sugimoto-Ishige, Y. Harada, Y. Adachi, Y. Usami, T. Kaji, K. Inoue, H. Hasegawa, T. Watanabe, A. Hijikata, et al. 2016. Protective neu-tralizing influenza antibody response in the absence of T follicular helper cells. *Nat. Immunol.* 17: 1447–1458.
15. Liu, Q., C. Fan, Q. Li, S. Zhou, W. Huang, L. Wang, C. Sun, M. Wang, X. Wu, J. Ma, et al. 2017. Antibody-dependent-cellular-cytotoxicity-inducing antibodies significantly affect the post-exposure treatment of Ebola virus infection. *Sci. Rep.* 7: 45552.
16. Pollara, J., D. Easterhoff, and G. G. Fouda. 2017. Lessons learned from human HIV vaccine trials. *Curr. Opin. HIV AIDS* 12: 216–221.
17. Snapper, C. M., and W. E. Paul. 1987. Interferon-gamma and B cell stimulatory factor-1 reciprocally regulate Ig isotype production. *Science* 236: 944–947.
18. Crotty, S. 2015. A brief history of T cell help to B cells. *Nat. Rev. Immunol.* 15: 185–189.
19. Stebegg, M., S. D. Kumar, A. Silva-Cayetano, V. R. Fonseca, M. A. Linterman, and L. Graca. 2018. Regulation of the germinal center response. *Front. Immunol.* 9: 2469.
20. Van-Dunem, J. C., L. C. Rodrigues, L. C. Alencar, M. F. Militão-Albuquerque, and R. A. Ximenes. 2015. Effectiveness of the first dose of BCG against tuber-culosis among HIV-infected, predominantly immunodeficient children. *BioMed Res. Int.* 2015: 275029.

21. Zwerling, A., M. A. Behr, A. Verma, T. F. Brewer, D. Menzies, and M. Pai. 2011. The BCG world Atlas: a database of global BCG vaccination policies and practices. *PLoS Med.* 8: e1001012.

22. Rouleau, M., A. Senik, E. Leroy, and J. P. Vernant. 1993. Long-term persistence of transferred PPD-reactive T cells after allogeneic bone marrow transplantation. *Transplantation* 55: 72–76.

23. Soares, A. P., C. K. Kwong Chung, T. Choice, E. J. Hughes, G. Jacobs, E. J. van Rensburg, G. Khomba, M. de Kock, L. Lerumo, L. Makhethe, et al. 2013. Longitudinal changes in CD4(+) T-cell memory responses induced by BCG vaccination of newborns. *J. Infect. Dis.* 207: 1084–1094.

24. Flynn, J. L., and J. Chan. 2001. Immunology of tuberculosis. *Annu. Rev. Immunol.* 19: 93–129.

25. Krutzik, S. R., and R. L. Modlin. 2004. The role of toll-like receptors in combating mycobacteria. *Semin. Immunol.* 16: 35–41.

26. Li, L., D. Qiao, X. Fu, S. Lao, X. Zhang, and C. Wu. 2011. Identification of *Mycobacterium tuberculosis*-specific Th1, Th17 and Th22 cells using the expression of CD40L in tuberculous pleurisy. *PLoS One* 6: e20165.

27. Salgame, P. 2005. Host innate and Th1 responses and the bacterial factors that control *Mycobacterium tuberculosis* infection. *Curr. Opin. Immunol.* 17: 374–380.

28. Khader, S. A., G. K. Bell, J. E. Pearl, J. J. Fountain, J. Rangel-Moreno, G. E. Cilley, F. Shen, S. M. Eaton, S. L. Gaffen, S. L. Swain, et al. 2007. IL-23 and IL-17 in the establishment of protective pulmonary CD4+ T cell responses after vaccination and during *Mycobacterium tuberculosis* challenge. *Nat. Immunol.* 8: 369–377.

29. Li, L., Y. Jiang, S. Lao, B. Yang, S. Yu, Y. Zhang, and C. Wu. 2016. Mycobacterium tuberculosis-specific IL-21+IFN-γ+CD4+ T cells are regulated by IL-12. *PLoS One* 11: e0147356.

30. Paidipally, P., D. Tripathi, A. Van, R. K. Radhakrishnan, R. Dhiman, S. Venkatasubramanian, K. P. Devalraju, A. R. Tvinnereim, V. L. Valluri, and R. Vankayalapati. 2018. Interleukin-21 regulates natural killer cell responses during *Mycobacterium tuberculosis* infection. *J. Infect. Dis.* 217: 1323–1333.

31. Roy Chowdhury, R., F. Vallania, Q. Yang, C. J. Lopez Angel, F. Darboe, A. Penn-Nicholson, V. Rozot, E. Nemes, S. T. Malherbe, K. Ronacher, et al. 2018. A multi-cohort study of the immune factors associated with M. tuberculosis infection outcomes. [Published erratum appears in 2018 *Nature* 564: E5.] *Nature* 560: 644–648.

32. Tamura, T., H. Ariga, T. Kinashi, S. Uehara, T. Kikuchi, M. Nakada, T. Tokunaga, W. Xu, A. Kariyone, T. Saito, et al. 2004. The role of antigenic peptide in CD4+ T helper phenotype development in a T cell receptor transgenic model. *Int. Immunol.* 16: 1691–1699.

33. Wolf, A. J., B. Linas, G. J. Trevejo-Nuñez, E. Kincaid, T. Tamura, K. Takatsu, and J. D. Ernst. 2007. *Mycobacterium tuberculosis* infects dendritic cells with high frequency and impairs their function in vivo. *J. Immunol.* 179: 2509–2519.

34. Bardarov, S., S. Bardarov, Jr., M. S. Pavelka, Jr., V. Sambandamurthy, M. Larsen, J. Tufariello, J. Chan, G. Hatfull, and W. R. Jacobs, Jr. 2002. Specialized transduction: an efficient method for generating marked and unmarked targeted gene disruptions in *Mycobacterium tuberculosis*, M. bovis BCG and M. smegmatis. *Microbiology* 148: 3007–3017.

35. Hatfull, G. F., and W. R. Jacobs, Jr. 2000. *Molecular Genetics of Mycobacteria*. ASM Press, Washington, DC.

36. Johnson, A. J., S. C. Kennedy, C. S. Lindestam Arlehamn, M. F. Goldberg, N. K. Saini, J. Xu, S. Paul, S. S. Hegde, J. S. Blanchard, J. Chan, et al. 2017. Identification of mycobacterial RplJ/L10 and RpsA/S1 proteins as novel targets for CD4⁺ T cells. *Infect. Immun.* 85: e01023.

37. Lutz, M. B., N. Kukutsch, A. L. Ogilvie, S. Rössner, F. Koch, N. Romani, and G. Schuler. 1999. An advanced culture method for generating large quantities of highly pure dendritic cells from mouse bone marrow. *J. Immunol. Methods* 223: 77–92.

38. Maecker, H. T., D. T. Umetsu, R. H. DeKruyff, and S. Levy. 1997. DNA vaccination with cytokine fusion constructs biases the immune response to ovalbumin. *Vaccine* 15: 1687–1696.

39. Zhao, Y., J. Ren, K. Harlos, D. M. Jones, A. Zeltina, T. A. Bowden, S. Padilla-Parra, E. E. Fry, and D. I. Stuart. 2016. Toremifene interacts with and destabilizes the Ebola virus glycoprotein. *Nature* 535: 169–172.

40. Aricescu, A. R., W. Lu, and E. Y. Jones. 2006. A time- and cost-efficient system for high-level protein production in mammalian cells. *Acta Crystallogr. D Biol. Crystallogr.* 62: 1243–1250.

41. Wec, A. Z., A. S. Herbert, C. D. Murin, E. K. Nyakatura, D. M. Abelson, J. M. Fels, S. He, R. M. James, M. A. de La Vega, W. Zhu, et al. 2017. Antibodies from a human survivor define sites of vulnerability for broad protection against Ebolaviruses. *Cell* 169: 878–890.e15.

42. Dauner, J. G., Y. Pan, A. Hildesheim, T. J. Kemp, C. Porras, and L. A. Pinto. 2012. Development and application of a GuHCl-modified ELISA to measure the avidity of anti-HPV L1 VLP antibodies in vaccinated individuals. *Mol. Cell. Probes* 26: 73–80.

43. Wec, A. Z., E. K. Nyakatura, A. S. Herbert, K. A. Howell, F. W. Holtsberg, R. R. Bakken, E. Mittler, J. R. Christin, S. Shulenin, R. K. Jangra, et al. 2016. A "Trojan horse" bispecific-antibody strategy for broad protection against ebolaviruses. *Science* 354: 350–354.

44. Wong, A. C., R. G. Sandesara, N. Mulherkar, S. P. Whelan, and K. Chandran. 2010. A forward genetic strategy reveals destabilizing mutations in the Ebolavirus glycoprotein that alter its protease dependence during cell entry. *J. Virol.* 84: 163–175.

45. Lalor, M. K., S. G. Smith, S. Floyd, P. Gorak-Stolinska, R. E. Weir, R. Blitz, K. Branson, P. E. Fine, and H. M. Dockrell. 2010. Complex cytokine profiles induced by BCG vaccination in UK infants. *Vaccine* 28: 1635–1641.

46. Prezzemolo, T., G. Guggino, M. P. La Manna, D. Di Liberto, F. Dieli, and N. Caccamo. 2014. Functional signatures of human CD4 and CD8 T cell responses to *Mycobacterium tuberculosis*. *Front. Immunol.* 5: 180.

47. Shan, G., T. Tang, H. Qian, and Y. Xia. 2018. Certain BCG-reactive responses are associated with bladder cancer prognosis. *Cancer Immunol. Immunother.* 67: 797–803.

48. Soares, A. P., T. J. Scriba, S. Joseph, R. Harbacheuski, R. A. Murray, S. J. Gelderbloem, A. Hawkridge, G. D. Hussey, H. Maecker, G. Kaplan, and W. A. Hanekom. 2008. *Bacillus* Calmette-Guérin vaccination of human newborns induces T cells with complex cytokine and phenotypic profiles. *J. Immunol.* 180: 3569–3577.

49. Breitfeld, D., L. Ohl, E. Kremmer, J. Ellwart, F. Sallusto, M. Lipp, and R. Förster. 2000. Follicular B helper T cells express CXC chemokine receptor 5, localize to B cell follicles, and support immunoglobulin production. *J. Exp. Med.* 192: 1545–1552.

50. Schaerli, P., K. Willimann, A. B. Lang, M. Lipp, P. Loetscher, and B. Moser. 2000. CXC chemokine receptor 5 expression defines follicular homing T cells with B cell helper function. *J. Exp. Med.* 192: 1553–1562.

51. D'Souza, S., V. Rosseels, M. Romano, A. Tanghe, O. Denis, F. Jurion, N. Castiglione, A. Vanonckelen, K. Palfliet, and K. Huygen. 2003. Mapping of murine Th1 helper T-Cell epitopes of mycolyl transferases Ag85A, Ag85B, and Ag85C from *Mycobacterium tuberculosis*. *Infect. Immun.* 71: 483–493.

52. Venkataswamy, M. M., M. F. Goldberg, A. Baena, J. Chan, W. R. Jacobs, Jr., and S. A. Porcelli. 2012. In vitro culture medium influences the vaccine efficacy of *Mycobacterium* bovis BCG. *Vaccine* 30: 1038–1049.

53. Bi, J., Y. Wang, H. Yu, X. Qian, H. Wang, J. Liu, and X. Zhang. 2017. Modulation of central carbon metabolism by acetylation of isocitrate lyase in *Mycobacterium tuberculosis*. *Sci. Rep.* 7: 44826.

54. Kunnath-Velayudhan, S., M. F. Goldberg, N. K. Saini, C. T. Johndrow, T. W. Ng, A. J. Johnson, J. Xu, J. Chan, W. R. Jacobs, Jr., and S. A. Porcelli. 2017. Transcriptome analysis of mycobacteria-specific CD4⁺ T cells identified by activation-induced expression of CD154. *J. Immunol.* 199: 2596–2606.

55. Ploegh, H. L. 2007. Bridging B cell and T cell recognition of antigen. *J. Immunol.* 179: 7193.

56. Arts, R. J. W., S. J. C. F. M. Moorlag, B. Novakovic, Y. Li, S. Y. Wang, M. Oosting, V. Kumar, R. J. Xavier, C. Wijmenga, L. A. B. Joosten, et al. 2018. BCG vaccination protects against experimental viral infection in humans through the induction of cytokines associated with trained immunity. *Cell Host Microbe* 23: 89–100.e5.

57. Kaufmann, E., J. Sanz, J. L. Dunn, N. Khan, L. E. Mendonça, A. Pacis, F. Tzelepis, E. Pernet, A. Dumaine, J. C. Grenier, et al. 2018. BCG educates hematopoietic stem cells to generate protective innate immunity against tuberculosis. *Cell* 172: 176–190.e19.

58. Checkley, A. M., D. H. Wyllie, T. J. Scriba, T. Golubchik, A. V. Hill, W. A. Hanekom, and H. McShane. 2011. Identification of antigens specific to non-tuberculous mycobacteria: the Mce family of proteins as a target of T cell immune responses. *PLoS One* 6: e26434.

59. Eivazi, S., S. Bagheri, M. S. Hashemzadeh, M. Ghalavand, E. S. Qamsari, R. Dorostkar, and M. Yasemi. 2016. Development of T follicular helper cells and their role in disease and immune system. *Biomed. Pharmacother.* 84: 1668–1678.

60. Lutwama, F., B. M. Kagina, A. Wajja, F. Waiswa, N. Mansoor, S. Kirimunda, E. J. Hughes, N. Kiwanuka, M. L. Joloba, P. Musoke, et al. 2014. Distinct T-cell responses when BCG vaccination is delayed from birth to 6 weeks of age in Ugandan infants. *J. Infect. Dis.* 209: 887–897.

61. Nemes, E., H. Geldenhuys, V. Rozot, K. T. Rutkowski, F. Ratangee, N. Bilek, S. Mabwe, L. Makhethe, M. Erasmus, A. Toefy, et al; C-040-404 Study Team. 2018. Prevention of *M. tuberculosis* infection with H4:IC31 vaccine or BCG revaccination. *N. Engl. J. Med.* 379: 138–149.

62. Pentel, P. R., D. H. Malin, S. Ennifar, Y. Hieda, D. E. Keyler, J. R. Lake, J. R. Milstein, L. E. Basham, R. T. Coy, J. W. Moon, et al. 2000. A nicotine conjugate vaccine reduces nicotine distribution to brain and attenuates its behavioral and cardiovascular effects in rats. *Pharmacol. Biochem. Behav.* 65: 191–198.

63. Lofano, G., F. Mancini, G. Salvatore, R. Cantisani, E. Monaci, C. Carrisi, S. Tavarini, C. Sammicheli, S. Rossi Paccani, E. Soldaini, et al. 2015. Oil-in-water emulsion MF59 increases germinal center B cell differentiation and persistence in response to vaccination. *J. Immunol.* 195: 1617–1627.

64. Spensieri, F., E. Siena, E. Borgogni, L. Zedda, R. Cantisani, N. Chiappini, F. Schiavetti, D. Rosa, F. Castellino, E. Montomoli, et al. 2016. Early rise of blood T follicular helper cell subsets and baseline immunity as predictors of persisting late functional antibody responses to vaccination in humans. *PLoS One* 11: e0157066.

65. Ko, E. J., Y. T. Lee, K. H. Kim, Y. J. Jung, Y. Lee, T. L. Denning, and S. M. Kang. 2016. Effects of MF59 adjuvant on induction of isotype-switched IgG antibodies and protection after immunization with T-dependent influenza virus vaccine in the absence of CD4+ T cells. *J. Virol.* 90: 6976–6988.